This PDF file includes:

Title
Author list
Author affiliations

Figures S1 to S11 and figure legends

Legends for Supplementary excel Supplementary Tables S1 to S10

Enhancing Proteasome Activity by NMDAR Antagonists Explains Their Therapeutic Effect in Neurodegenerative and Mental Diseases

Fikret Sahin[1]*, Aslihan Gunel[2], Buse Turegun Atasoy[1], Ulku Guler[3], Bekir Salih[3], Isunsu Kuzu[4], Mehmet Taspinar[5], Ozgur Cinar[6], Selda Kahveci[6]

[1] Ankara University School of Medicine, Department of Medical Microbiology, Ankara, Turkey

[2] Kırşehir Ahi Evran University, Faculty of Arts and Science Department of Chemistry-Biochemistry

[3] Hacettepe University, Department of Chemistry

[4] Ankara University School of Medicine, Department of Medical Pathology, Ankara, Turkey

[5] Aksaray University School of Medicine, Department of Medical Biology, Aksaray, Turkey

[6]Ankara University School of Medicine, Department of Histology and Embryology, Ankara, Turkey

***Corresponding author. Fikret Şahin, Email: fsahin29@hotmail.com**

Figures

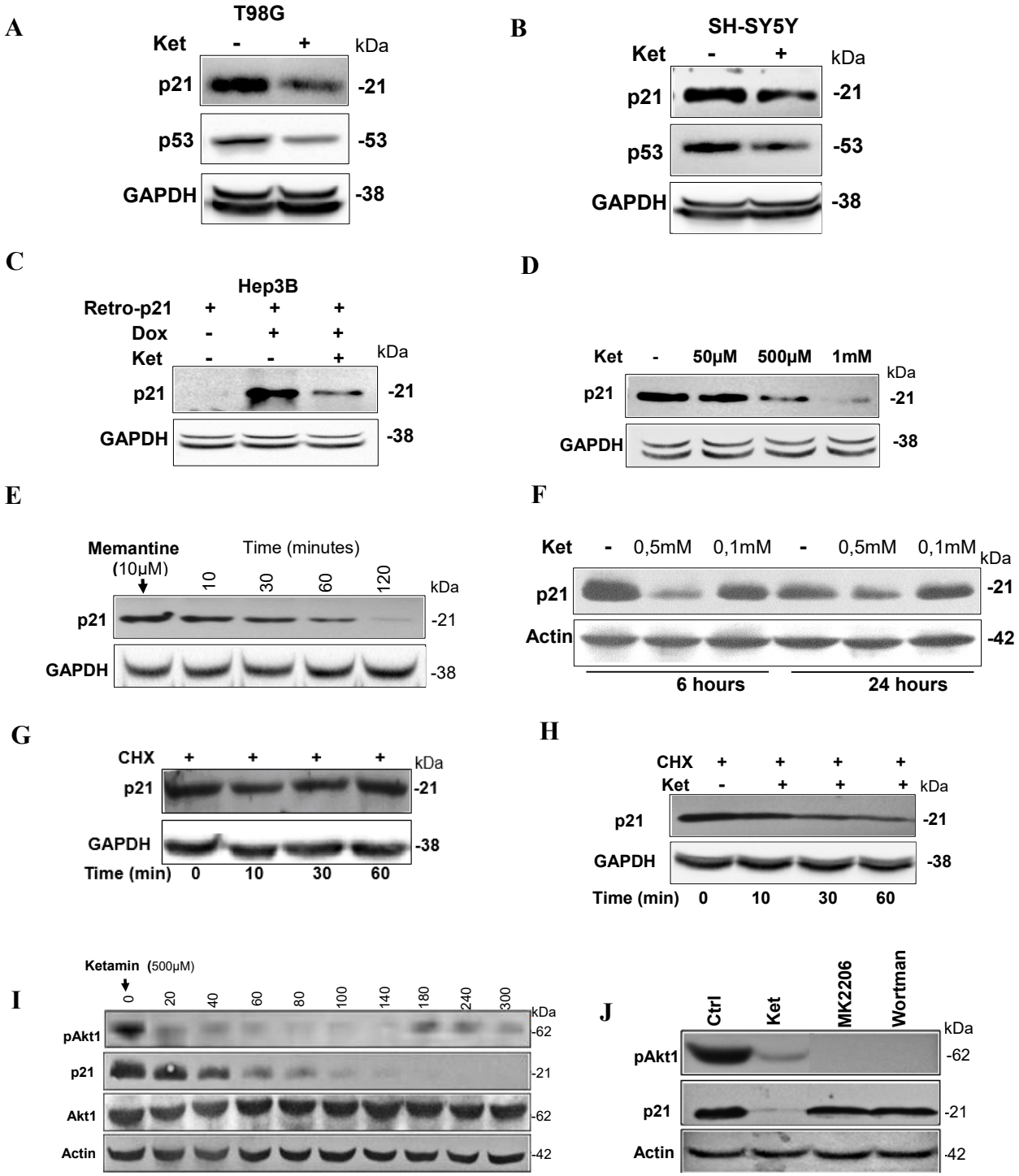
A
T98G
Ket - +
kDa
p21 -21
p53 -53
GAPDH -38
B
SH-SY5Y
Ket - +
kDa
p21 -21
p53 -53
GAPDH -38
C
Hep3B
Retro-p21 + + +
Dox - + +
Ket - - +
kDa
p21 -21
GAPDH -38
D
Ket - 50μM 500μM 1mM
kDa
p21 -21
GAPDH -38
E
Memantine (10μM)
Time (minutes)
10 30 60 120
kDa
p21 -21
GAPDH -38
F
Ket - 0,5mM 0,1mM - 0,5mM 0,1mM
kDa
p21 -21
Actin -42
6 hours
24 hours
G
CHX + + + +
kDa
p21 -21
GAPDH -38
Time (min) 0 10 30 60
H
CHX + + + +
Ket - + + +
kDa
p21 -21
GAPDH -38
Time (min) 0 10 30 60
I
Ketamin (500μM)
0 20 40 60 80 100 140 180 240 300
kDa
pAkt1 -62
p21 -21
Akt1 -62
Actin -42
J
Ctrl
Ket
MK2206
Wortman
kDa
pAkt1 -62
p21 -21
Actin -42

Fig. S1 Rapid reduction of IDP-characteristic proteins by NMDAR antagonists across cell lines.
(**A-C**) Demonstrated decrease in p21 protein levels by ketamine treatment in various cell lines. Hep3B, lacking detectable p21, was supplemented with ectopically expressed p21 via the dox inducible RetroPur vector system. This reduction is (**D**) dose-dependent, (**E, F**) time-dependent, and (**G, H**) not prevented by cycloheximide, suggesting direct degradation rather than inhibited synthesis. (**I**) ketamine decrease phosphorylated Akt1 (**J**) MK-2206, an Akt1 phosphorylation inhibitor at serine 473, and wortmannin, a specific PI3K inhibitor (an upstream kinase of Akt1) reduced phosphorylated Akt1 levels, they did not diminish p21 levels as substantially as the NMDAR antagonists. All unprocessed and uncropped gel and blot images are available in the supplementary file titled "Unprocessed Gel Blots".

A

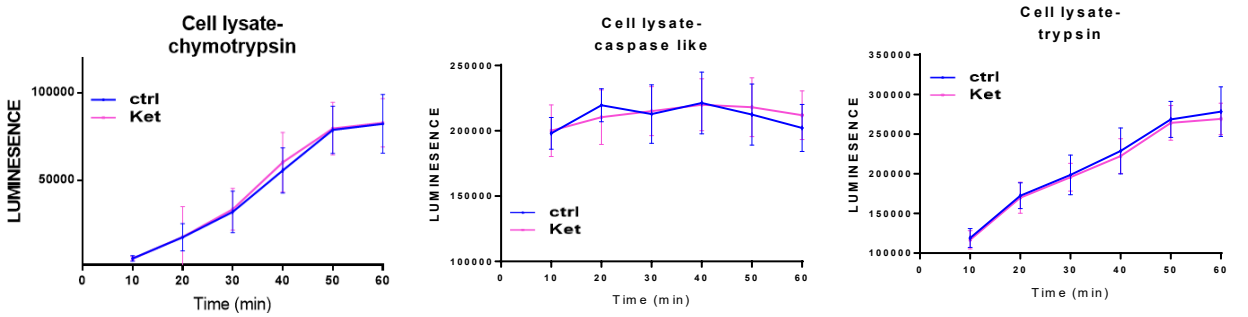

B

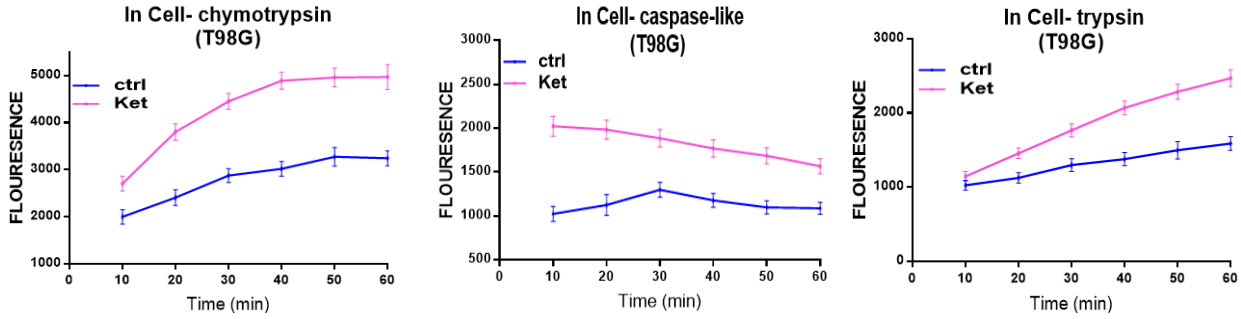

C

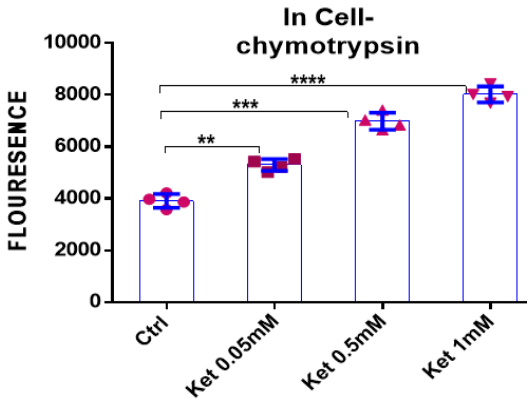

D

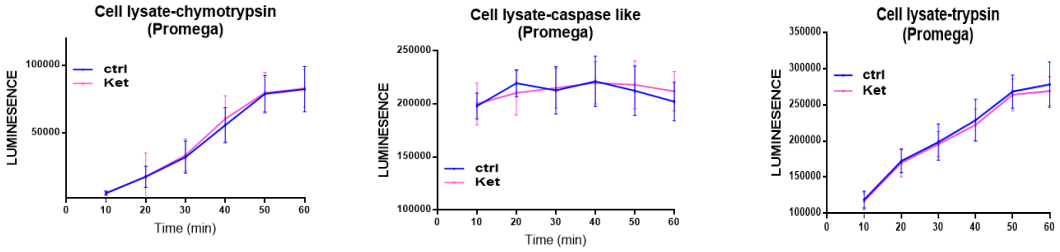
Cell lysate-chymotrypsin (Promega)
Cell lysate-caspase like (Promega)
Cell lysate-trypsin (Promega)
LUMINESCENCE
ctrl
Ket
Time (min)

E

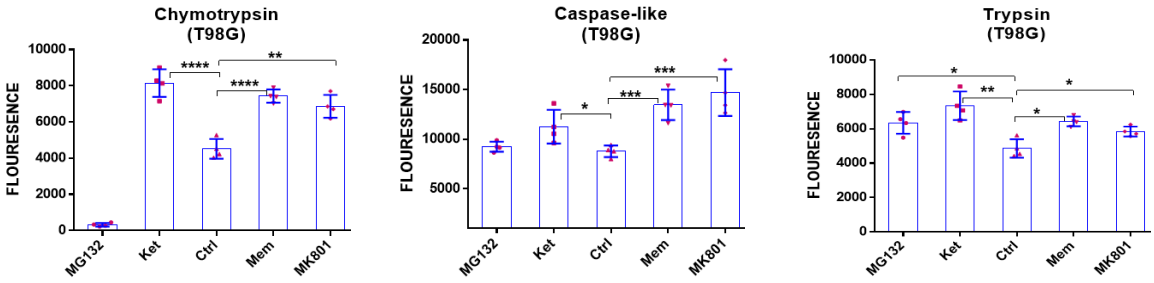
Chymotrypsin (T98G)
Caspase-like (T98G)
Trypsin (T98G)
FLOURESCENCE
MG132
Ket
Ctrl
Mem
MK801

F

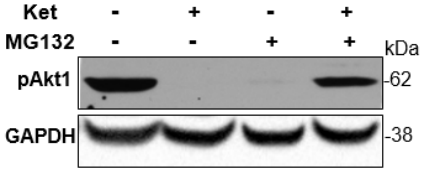
Ket
MG132
kDa
pAkt1
GAPDH
-62
-38

G

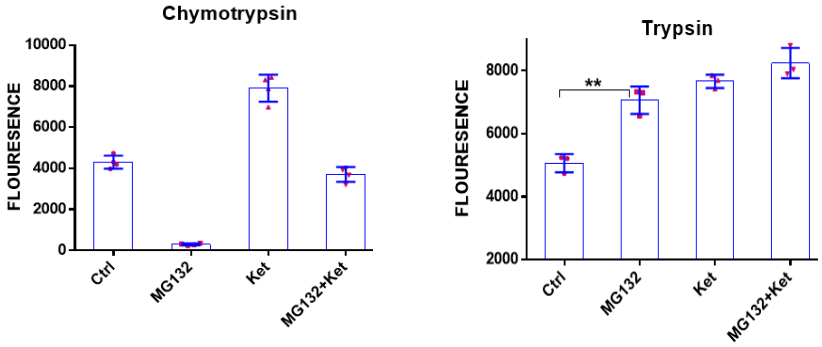
Chymotrypsin
Trypsin
FLOURESCENCE
Ctrl
MG132
Ket
MG132+Ket

H

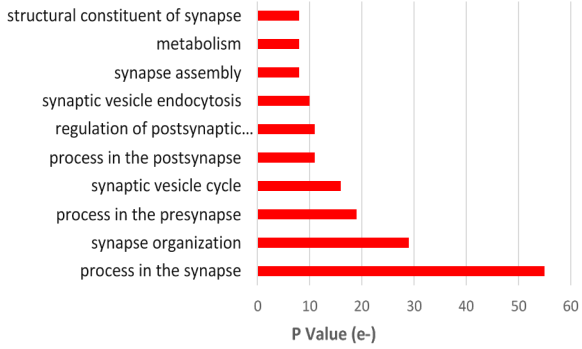
Enrichment of 145 increased proteins with SynGO-Biological process terms
structural constituent of synapse
metabolism
synapse assembly
synaptic vesicle endocytosis
regulation of postsynaptic...
process in the postsynapse
synaptic vesicle cycle
process in the presynapse
synapse organization
process in the synapse
P Value (e-)

I

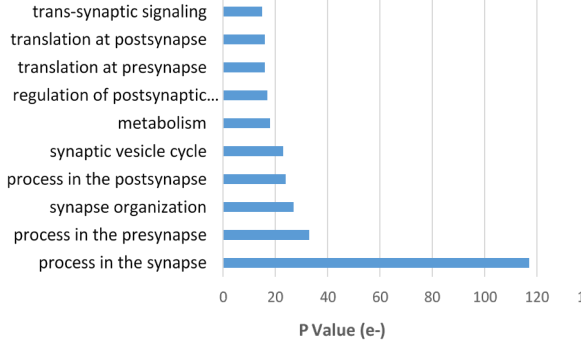
Enrichment of 372 decreased proteins with SynGO-Biological process terms
trans-synaptic signaling
translation at postsynapse
translation at presynapse
regulation of postsynaptic...
metabolism
synaptic vesicle cycle
process in the postsynapse
synapse organization
process in the presynapse
process in the synapse
P Value (e-)

Fig. S2 NMDAR antagonist-induced proteasome activity changes and synaptic protein alterations:
(**A**) Applying fluorogenic substrates to cell lysates of HepG2, Hep3B, T98G, and SH-SY5Y as conventional methods demonstrated that ketamine did not alter the chymotrypsin, trypsin, or caspase-like activities of the proteasome. (**B**) Using the "In-Cell Fluorogenic Proteasome Assay," NMDAR antagonists were found to increase chymotrypsin-like, caspase-like, and trypsin-like proteasome activities in T98G cells. (**C**) dose-dependent enhancement of chymotrypsin-like activity by ketamine. (**D**) The chymotrypsin, caspase-like, and trypsin activities in cell lysate of HepG2 cell were assessed using the "Cell-Based Proteasome Luciferase Systems" (Promega). (**E**) varied effects on proteasome activities by different NMDAR antagonists and proteasome inhibitor MG132 in T98G cells. (**F**) The proteasome inhibitor MG132 has no effect on the decrease of pAkt1 in the presence of ketamine (**G**) Selective inhibition of chymotrypsin-like activity by MG132, without affecting trypsin or caspase-like activities. (**H, I**) SynGO biological terms analysis of proteins with decreased (372) and increased (145) abundance. Results are presented as mean ± SEM. * denotes $p < 0.05$, ** denotes $p < 0.01$, and *** denotes $p < 0.001$ for comparisons between drugs results against controls. P values were calculated using a two-tailed unpaired t-test to compare the control group with the individual chemical effect. Western blot analyses were performed on independent biological samples with the entire procedure replicated at least twice to confirm consistency of the results. All unprocessed and uncropped gel and blot images are available in the supplementary file titled "Unprocessed Gel Blots".

A

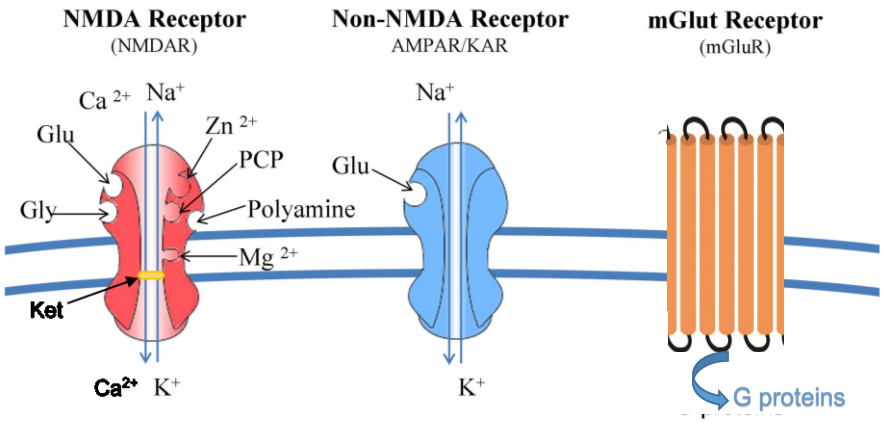

Fig. S3. Mapping of glutamate receptors and their respective binding sites.

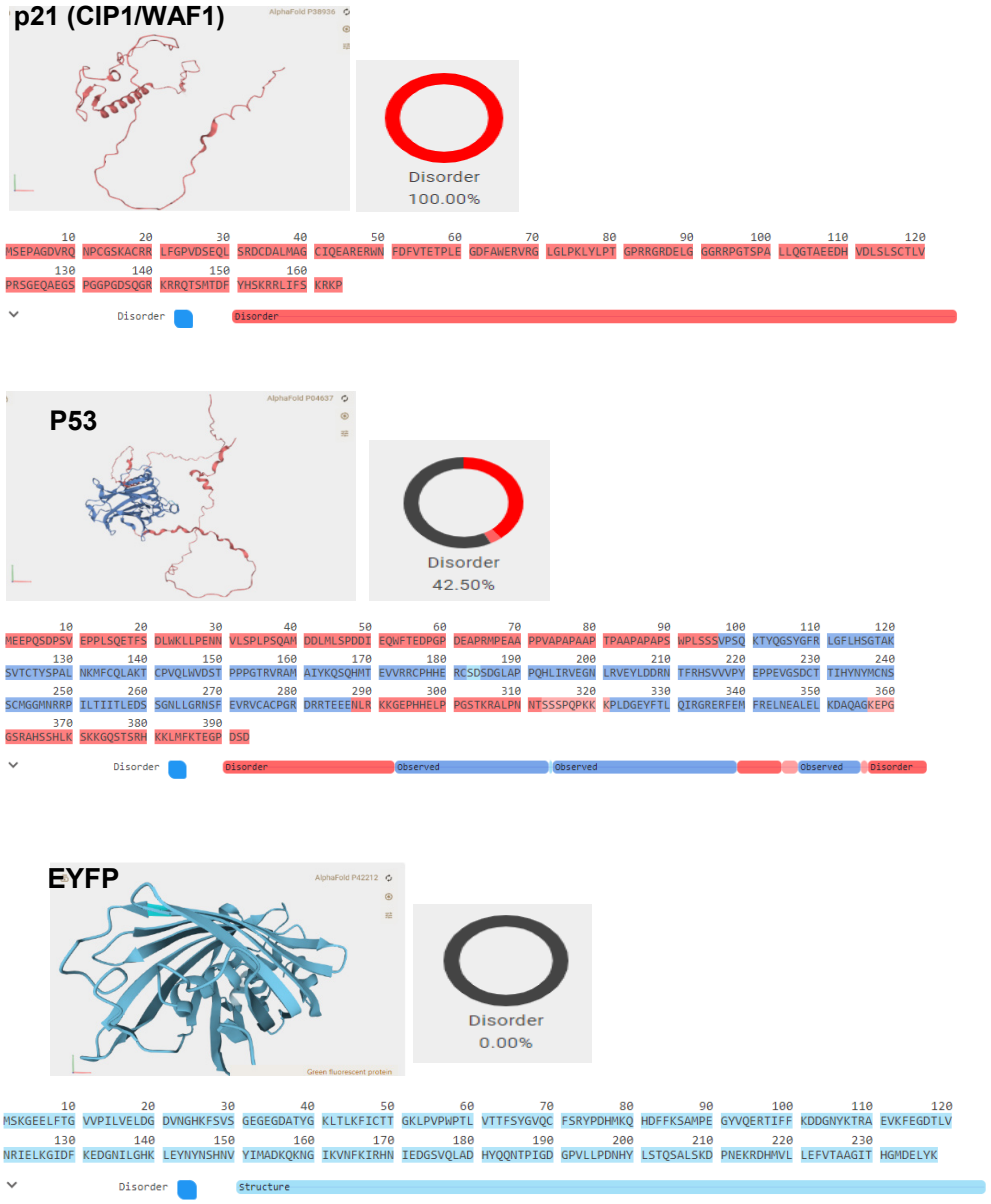

Fig. S4. The amounts of intrinsically disordered regions in p21, p53, and EYFP proteins are presented (AlphaFold-disorder (https://alphafold.ebi.ac.uk/).

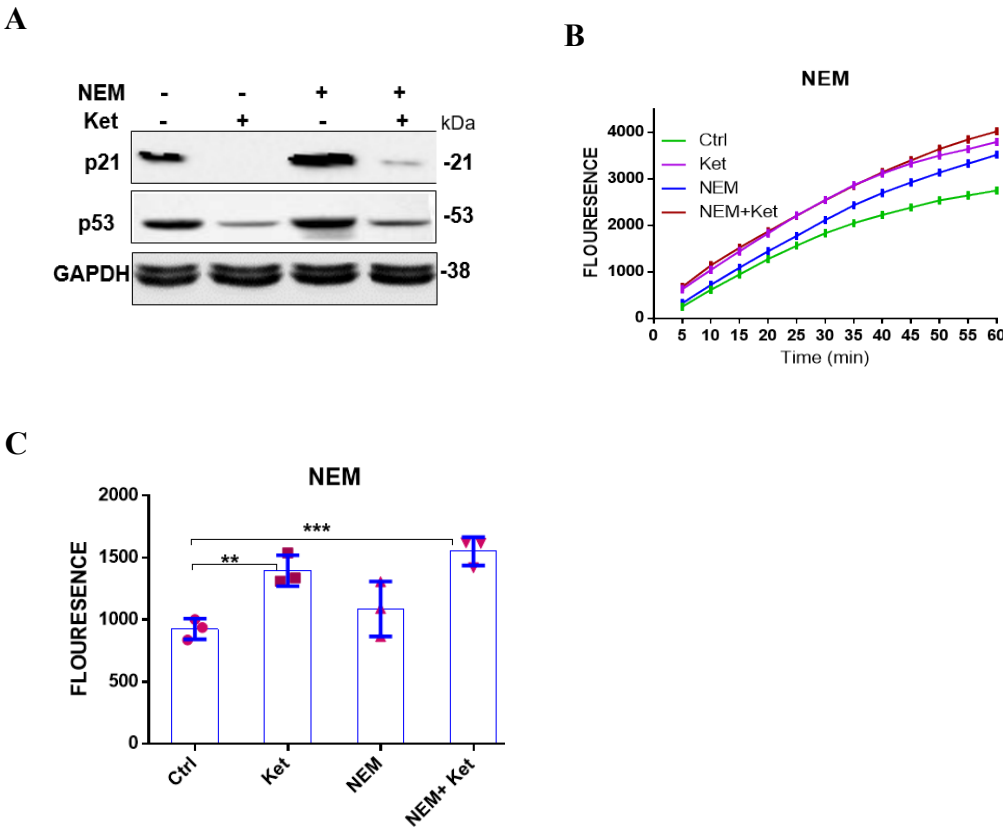

Fig. S5. Exploration of the DUB enzymes USP14 and UCHL5 regarding NMDAR antagonist impact. (**A**) Analysis of p21 protein response to the USP14 and UCHL5 inhibitor N-Ethylmaleimide (NEM) (10µM-6h incubation) and to ketamine in NEM's presence. (**B, C**) Investigation of NEM effects on chymotrypsin-like activity and ketamine's impact on this activity when co-treated with NEM. Results are presented as the mean ± SEM, based on 3 technical replicates from each of n = 3 independent experiment. *Asterisks denote significance levels: *p < 0.05, **p < 0.01, ***p < 0.001. P values were calculated using a two-tailed unpaired t-test to compare the control group with the individual chemical effect. All unprocessed and uncropped gel and blot images are available in the supplementary file titled "Unprocessed Gel Blots".

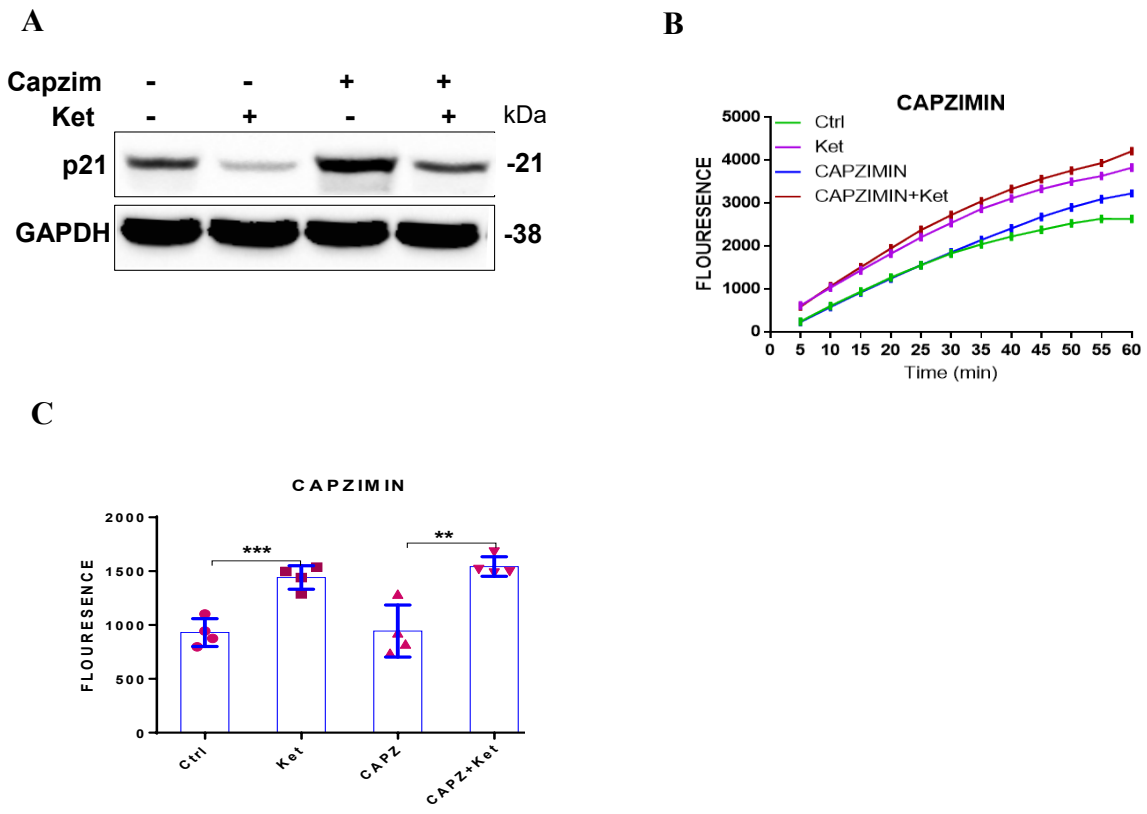

Fig. S6. Evaluation of the DUB enzyme RPN11 (PSMD14) regarding NMDAR antagonist effects. (**A**) Assessment of p21 protein levels following treatment with the PSMD14 inhibitor capzimin (10µM, 6h incubation) and subsequent ketamine exposure in the presence of capzimin. (**B, C**) Investigation into the impact of capzimin on chymotrypsin-like proteasome activity and its alteration in the context of ketamine treatment when combined with capzimin. Results are presented as the mean ± SEM, based on 4 technical replicates from each of n = 3 independent experiment. *Asterisks denote significance levels: *p < 0.05, **p < 0.01, ***p < 0.001. P values were calculated using a two-tailed unpaired t-test to compare the control group with the individual chemical effect. All unprocessed and uncropped gel and blot images are available in the supplementary file titled “Unprocessed Gel Blots”.

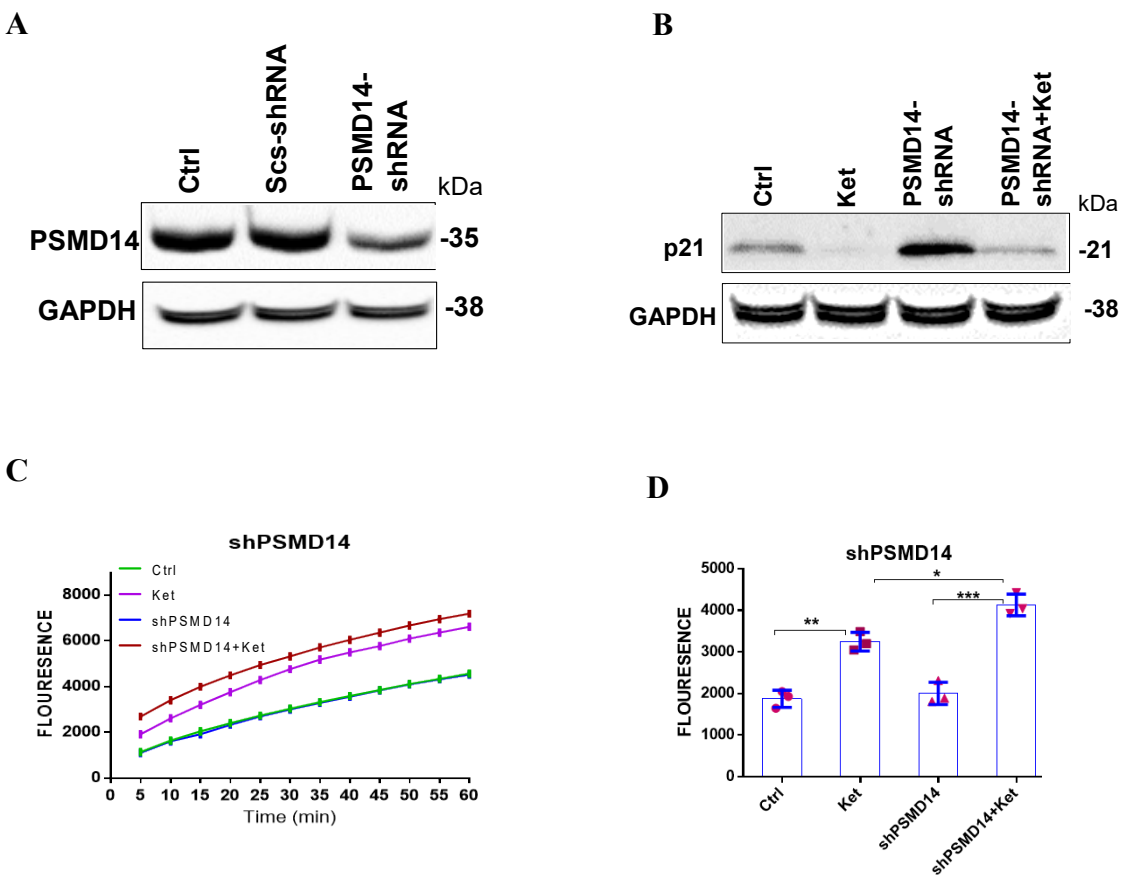

Fig. S7. Analysis of RPN11 (PSMD14) silencing on proteasome activity in NMDAR antagonist contexts in HepG2 and T98G cell lines. (**A**) PSMD14 knockdown in HepG2 cells.(**B**) Ketamine influence on p21 protein levels in PSMD14-silenced versus control cells. (**C, D**) Assessment of ketamine's impact on chymotrypsin-like activity in PSMD14-knockdown compared to control cells. Results are presented as the mean ± SEM, based on 3 technical replicates from each of n = 3 independent experiment. *Asterisks denote significance levels: *p < 0.05, **p < 0.01, ***p < 0.001. P values were calculated using a two-tailed unpaired t-test to compare the control group with the PSMD14 knockdown cells. All unprocessed and uncropped gel and blot images are available in the supplementary file titled “Unprocessed Gel Blots”.

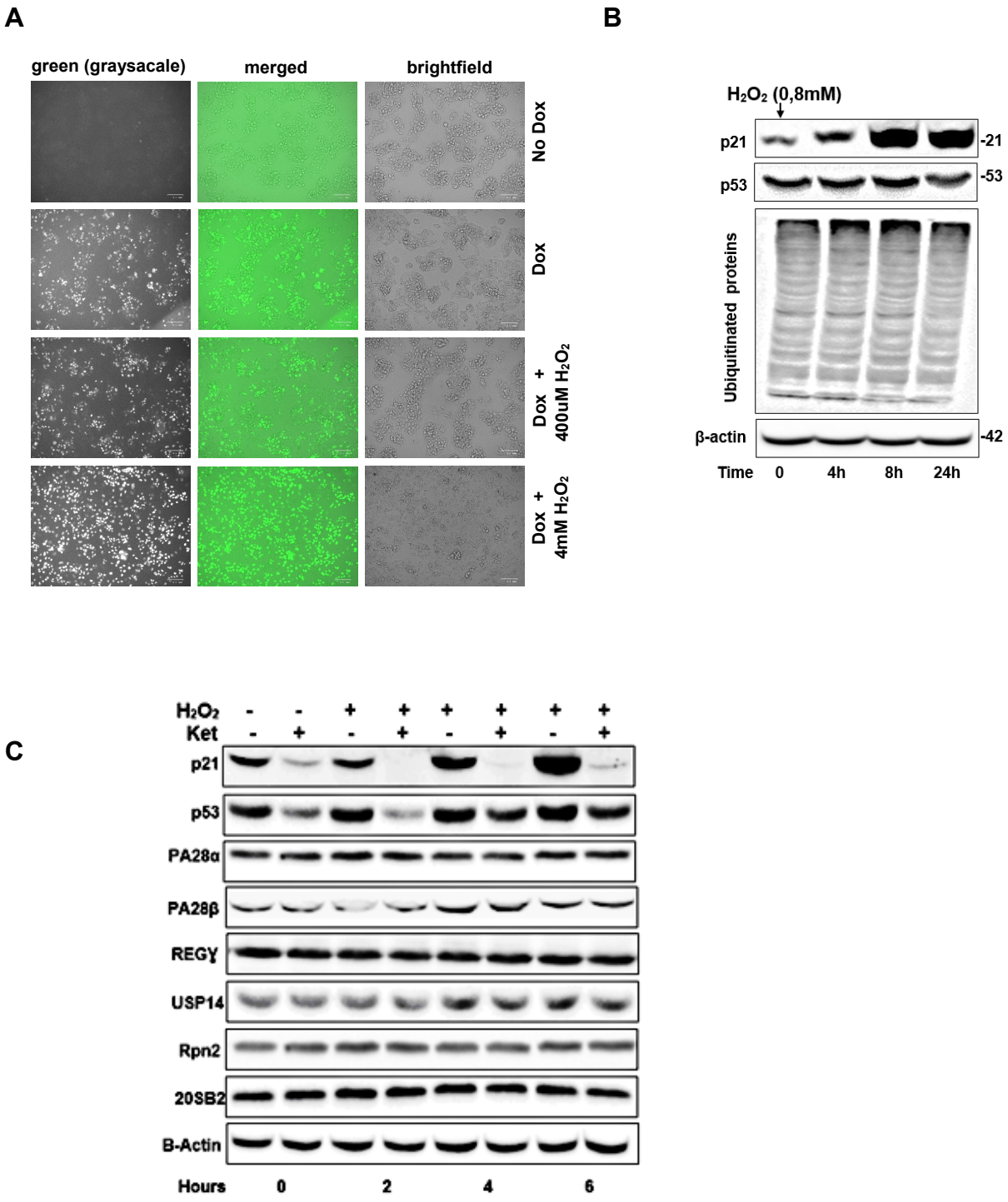

Fig. S8. Evaluation of H_2O_2 and ketamine effects on cell cycle and proteasome regulatory proteins. (**A**) Analysis of p21-GFP protein levels under different H_2O_2 concentrations. (**B**) Time-course study of p21, p53, and total ubiquitin levels in response to 800 µM H_2O_2 concentrations over 24 hours. (**C**) Investigation of ketamine's influence on the cell cycle proteins p21, p53, and proteasome regulatory proteins (28α, 28β, 28Ɣ, 20S core protein 20Sb2, USP14, Rpn2) during 800 µM H_2O_2 treatment. All unprocessed and uncropped gel and blot images are available in the supplementary file titled “Unprocessed Gel Blots”.

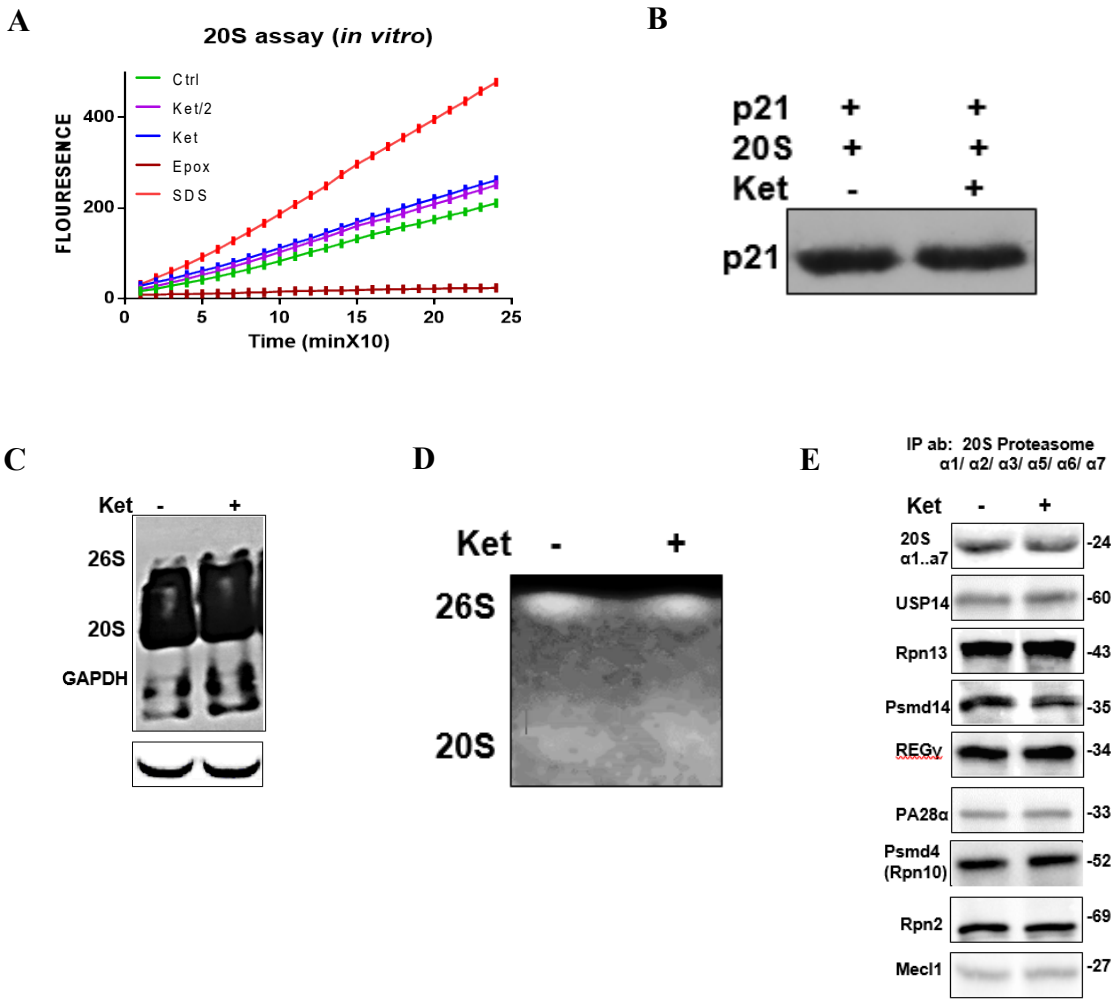

Fig. S9. Analysis of ketamine's effects on proteasome structures and functions. (**A**) Measurement of 20S proteasome activity in response to ketamine using the Enzo Life Sciences 20S Proteasome Assay Kit, with SDS activation and Epoxomicin inhibition according to kit protocols. (**B**) Assessment of ketamine's influence on the 20S proteasome-mediated degradation of His-tagged p21 protein using the purified 20S proteasome from the assay kit. (**C, D**) Characterization of structural changes in 26S and 20S complexes induced by ketamine via native gel electrophoresis and Wb with α1–α7 antibodies. (**E**) Evaluation of interactions between 20S core subunit proteins (α1−α7) and 19S/20S regulatory proteins (USP14, Rpn13, Psmd14, Psmd4, Rpn2, RegɣV, PA28α, Lmp2, Mecl1) through co-immunoprecipitation in ketamine-treated and untreated cells. All unprocessed and uncropped gel and blot images are available in the supplementary file titled “Unprocessed Gel Blots”.

A

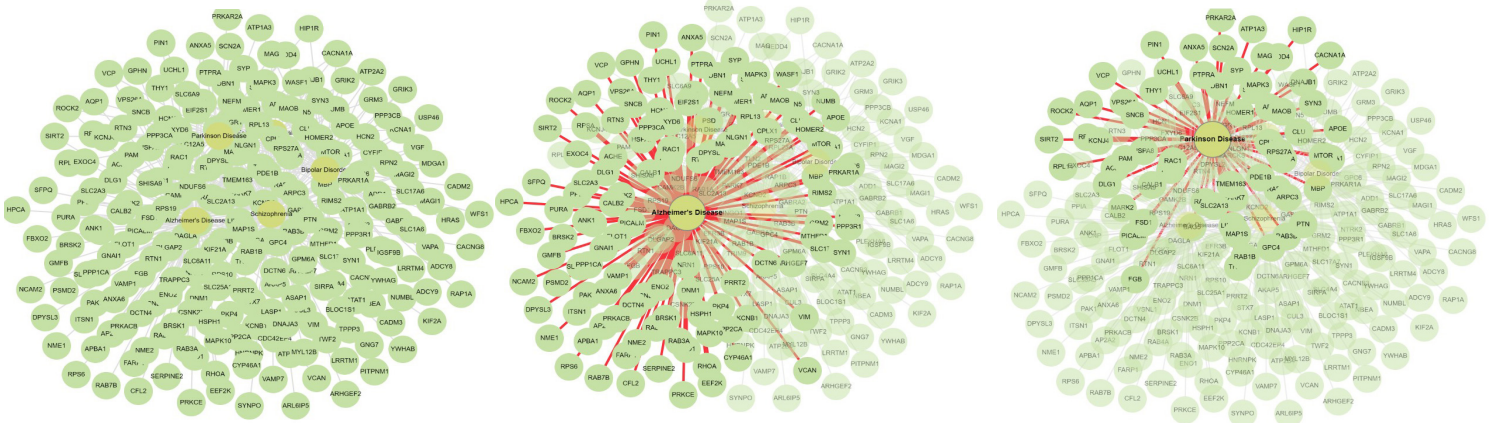

B

ALZHEİMER'S DISEASE KEGG PATHWAY

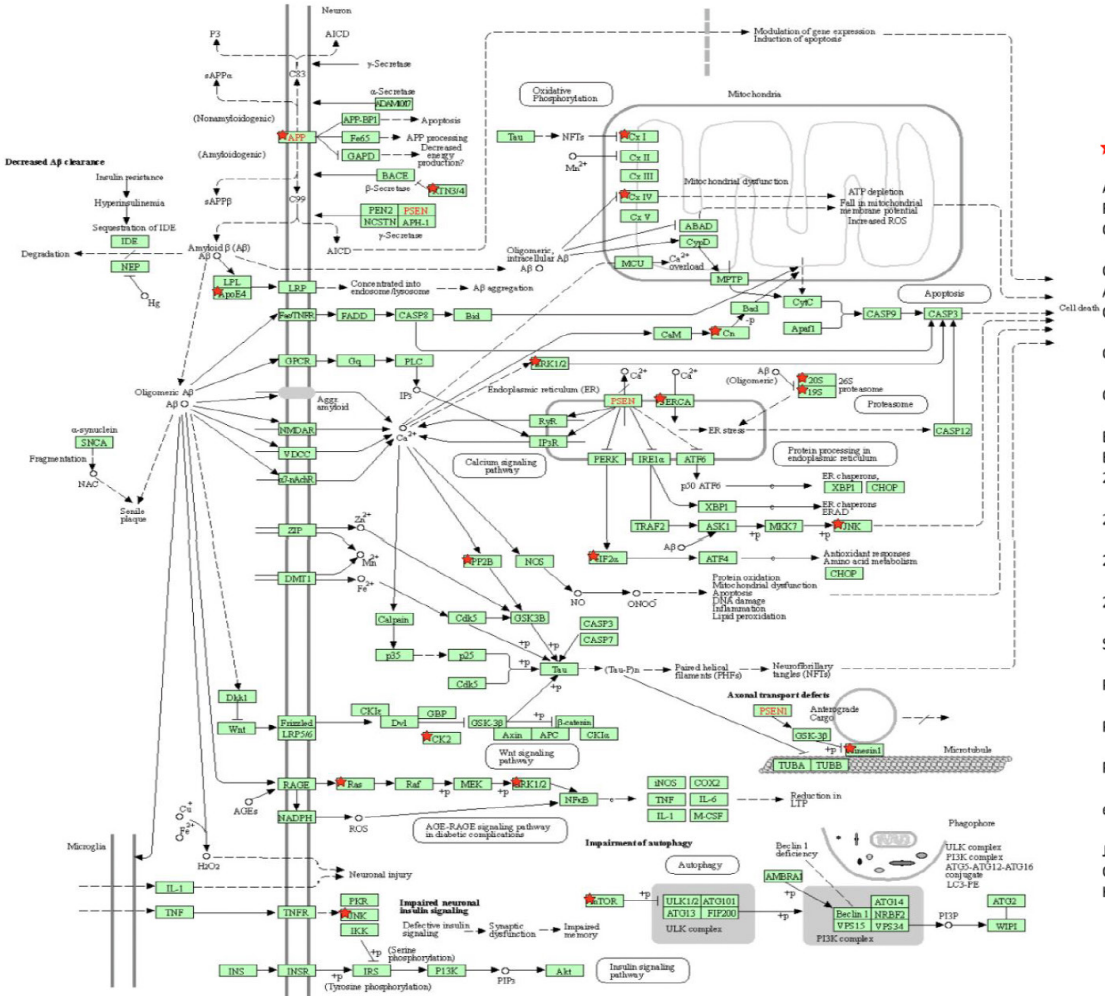

★	Alzheimer's Disease -related proteins changed in the study	Short name
APP	amyloid beta (A4) precursor protein	APP
RTN3/4	reticulon 3 and 4	RTN
CX I	NADH:ubiquinone oxidoreductase core subunit S6	Ndufs6
CX V-	NADH:ubiquinone oxidoreductase subunit A7	Ndufa7
Apoe4	apolipoprotein E	Apoe
Cn	protein phosphatase 3, catalytic subunit, alpha isoform	Ppp3ca
Cn	protein phosphatase 3, catalytic subunit, beta isoform	Ppp3cb
Cn	protein phosphatase 3, regulatory subunit B, alpha isoform (calcineurin B, type I)	Ppp3r1
ERK1/2	mitogen-activated protein kinase 3	Mapk3
ERK1/2	mitogen-activated protein kinase 10	Mapk10
20S	proteasome (prosome, macropain) subunit, beta type 4	Psmb4
26S	proteasome (prosome, macropain) 26S subunit, non-ATPase, 2	Psmd2
26S	proteasome (prosome, macropain) 26S subunit, non-ATPase, 2	Psmd7
26S	proteasome (prosome, macropain) 26S subunit, non-ATPase, 2	Psmd12
SERCA	ATPase, Ca++ transporting, cardiac muscle, fast twitch 1	Atp2a2
PP2B	protein phosphatase 3, catalytic subunit, alpha isoform	Ppp3ca
PP2B	protein phosphatase 3, catalytic subunit, beta isoform	Ppp3cb
PP2B	protein phosphatase 3, regulatory subunit B, alpha isoform (calcineurin B, type I)	Ppp3r1
eIF2A	eukaryotic translation initiation factor 2, subunit 1 alpha	Eif2s1
JNK	mitogen-activated protein kinase 10	Mapk10
CK2	casein kinase 2, beta polypeptide	Csnk2b
Kinesin1	kinesin family member 5B	Kif5b

C

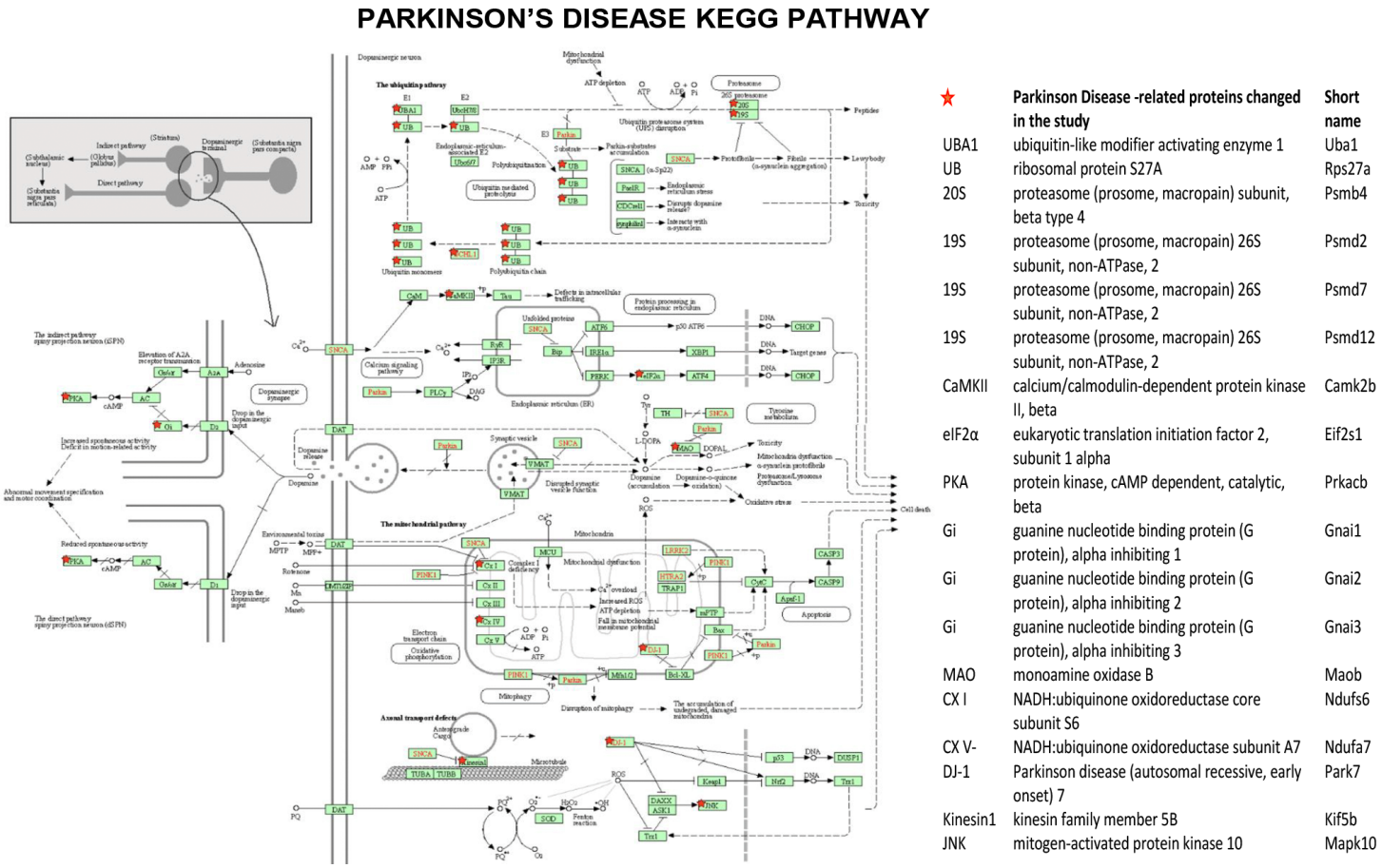

★	Parkinson Disease -related proteins changed in the study	Short name
UBA1	ubiquitin-like modifier activating enzyme 1	Uba1
UB	ribosomal protein S27A	Rps27a
20S	proteasome (prosome, macropain) subunit, beta type 4	Psmb4
19S	proteasome (prosome, macropain) 26S subunit, non-ATPase, 2	Psmd2
19S	proteasome (prosome, macropain) 26S subunit, non-ATPase, 2	Psmd7
19S	proteasome (prosome, macropain) 26S subunit, non-ATPase, 2	Psmd12
CaMKII	calcium/calmodulin-dependent protein kinase II, beta	Camk2b
eIF2α	eukaryotic translation initiation factor 2, subunit 1 alpha	Eif2s1
PKA	protein kinase, cAMP dependent, catalytic, beta	Prkacb
Gi	guanine nucleotide binding protein (G protein), alpha inhibiting 1	Gnai1
Gi	guanine nucleotide binding protein (G protein), alpha inhibiting 2	Gnai2
Gi	guanine nucleotide binding protein (G protein), alpha inhibiting 3	Gnai3
MAO	monoamine oxidase B	Maob
CX I	NADH:ubiquinone oxidoreductase core subunit S6	Ndufs6
CX V-	NADH:ubiquinone oxidoreductase subunit A7	Ndufa7
DJ-1	Parkinson disease (autosomal recessive, early onset) 7	Park7
Kinesin1	kinesin family member 5B	Kif5b
JNK	mitogen-activated protein kinase 10	Mapk10

Fig. S10. Characterization of protein alterations and their relation to neurodegenerative disease pathways. (**A**) Utilization of the Enrichr-KG database for the 517 altered proteins identifies associations with diseases like AD and PD. (**B**) KEGG pathway enrichment for Alzheimer's Disease evidences various implicated etiologies linked to the altered proteins [45,46]. (**C**) Enrichment in the Parkinson's Disease KEGG pathway highlights connections to multiple PD etiologies involving the 517 altered proteins. Proteins denoted by red stars are detailed in the accompanying table [45,46].

A

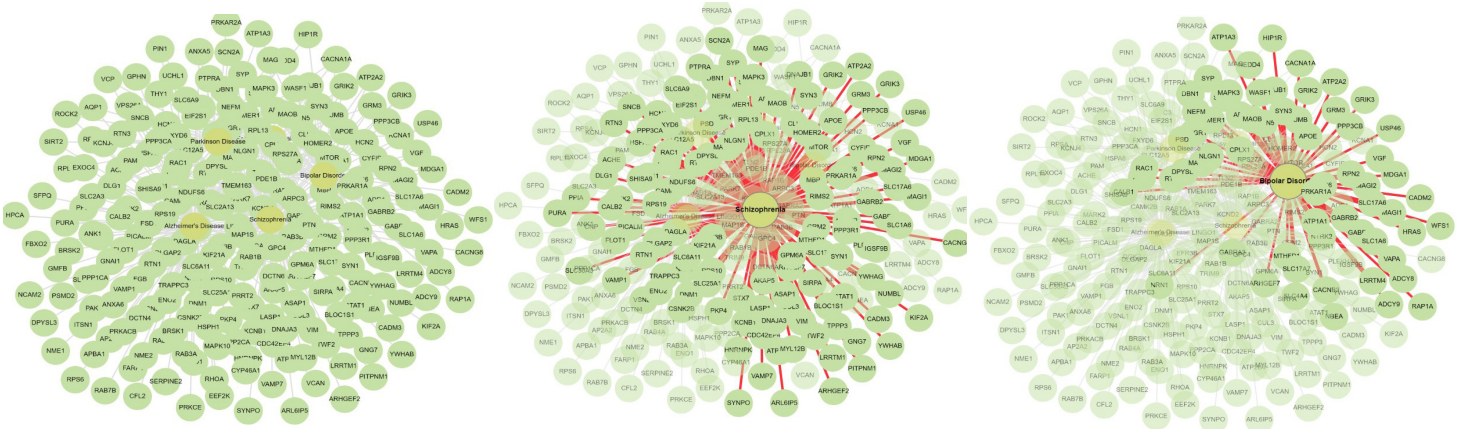
Schizophrenia
Bipolar Disorder

B

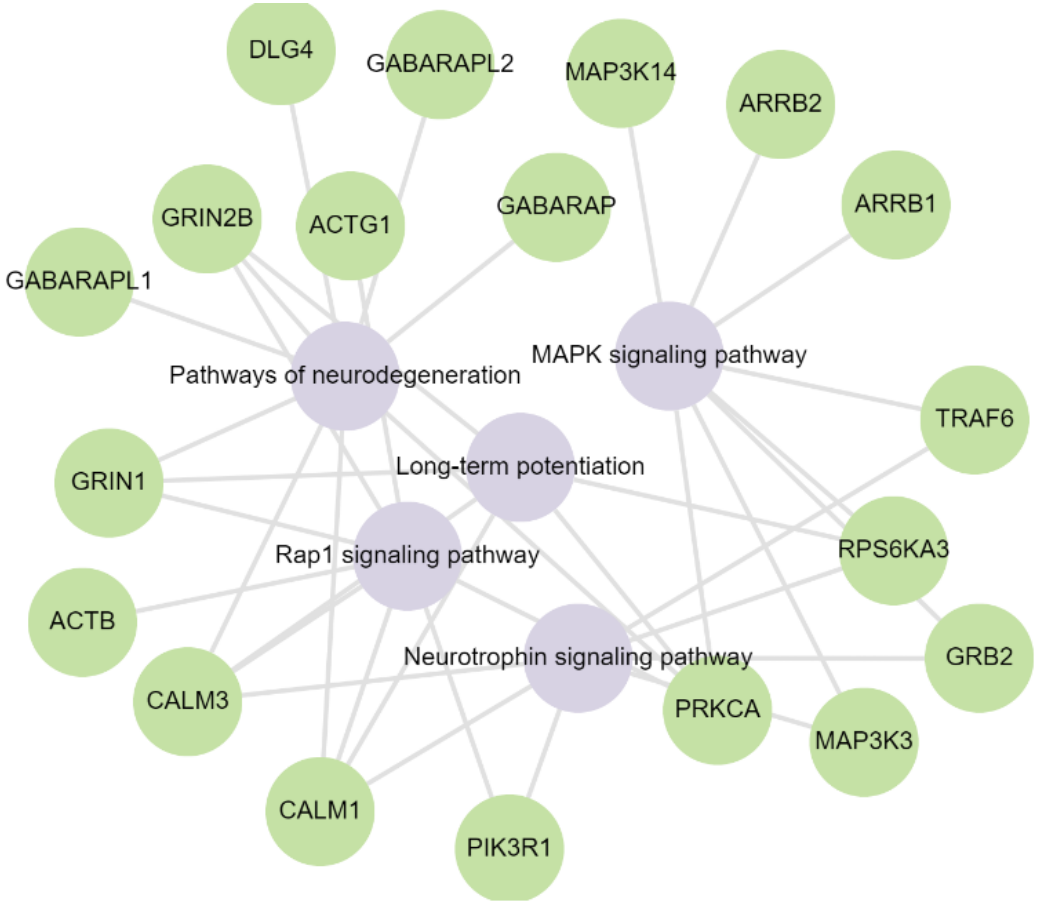
DLG4
GABARAPL2
MAP3K14
ARRB2
GRIN2B
ACTG1
GABARAP
ARRB1
GABARAPL1
Pathways of neurodegeneration
MAPK signaling pathway
TRAF6
GRIN1
Long-term potentiation
Rap1 signaling pathway
RPS6KA3
ACTB
Neurotrophin signaling pathway
GRB2
CALM3
PRKCA
MAP3K3
CALM1
PIK3R1

C

retrograde endocannabinoid signaling KEGG Pathway

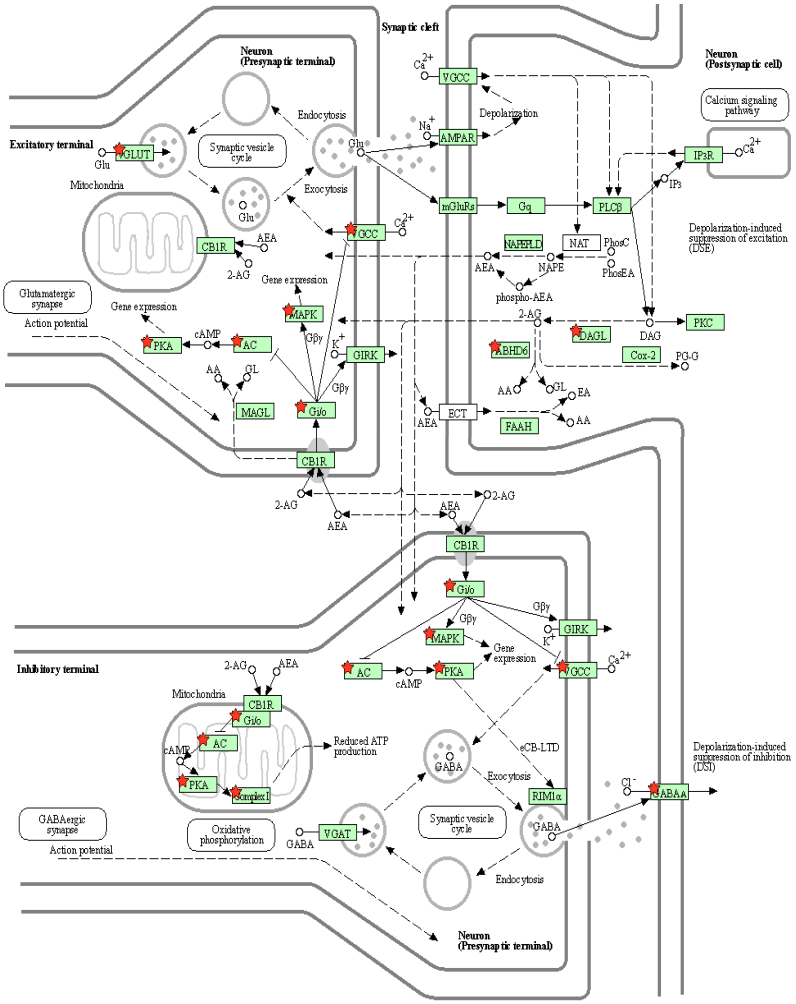

★	Retrograde ennocanno -related proteins changed in the study	Short name
VGLUT	solute carrier family 17 (sodium-dependent inorganic phosphate cotransporter), member 6	SLC17A6
VGLUT	solute carrier family 17 (sodium-dependent inorganic phosphate cotransporter), member 7	SLC17A7
VGLUT	solute carrier family 17 (sodium-dependent inorganic phosphate cotransporter), member 8	SLC17A8
VGGC	calcium channel, voltage-dependent, P/Q type, alpha 1A subunit	CACNA1A
PKA	protein kinase, cAMP dependent, catalytic, beta	PRKACB
AC	adenylate cyclase 8	ADCY8
AC	adenylate cyclase 9	ADCY9
ABHD6	abhydrolase domain containing 6	ABHD6
DAGL	diacylglycerol lipase, alpha	DAGLA
Gi/o	guanine nucleotide binding protein (G protein), alpha inhibiting 1	GNAI1
Gi/o	guanine nucleotide binding protein (G protein), alpha inhibiting 2	GNAI2
Gi/o	guanine nucleotide binding protein (G protein), alpha inhibiting 3	GNAI3
Gi/o	guanine nucleotide binding protein (G protein), gamma 7	GNG7
Complex1	NADH:ubiquinone oxidoreductase core subunit S6	NDUFS6
Complex1	NADH:ubiquinone oxidoreductase core subunit S7	NDUFS7
$GABA_A$	gamma-aminobutyric acid (GABA) A receptor, subunit alpha 2	GABRA2
$GABA_A$	gamma-aminobutyric acid (GABA) A receptor, subunit alpha 3	GABRA3
$GABA_A$	gamma-aminobutyric acid (GABA) A receptor, subunit beta 1	GABRB1
$GABA_A$	gamma-aminobutyric acid (GABA) A receptor, subunit beta 2	GABRB2

D

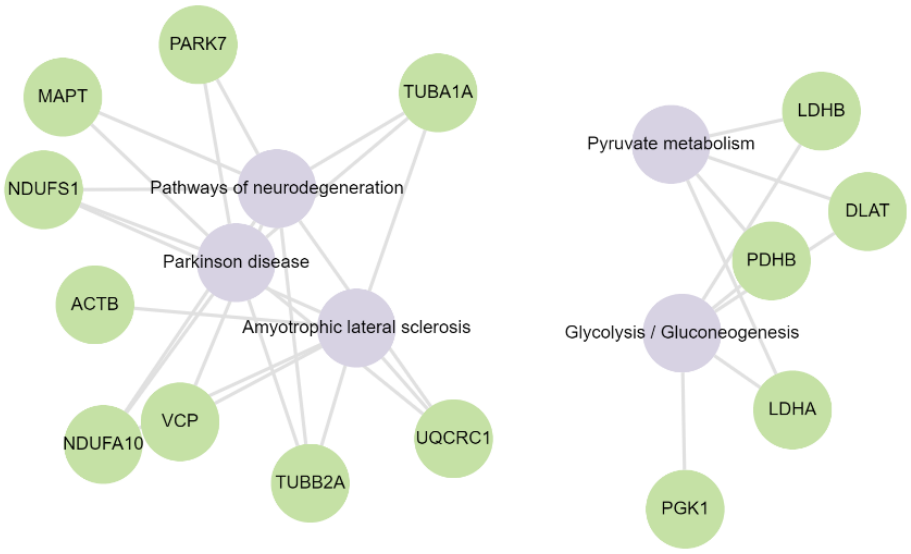

E

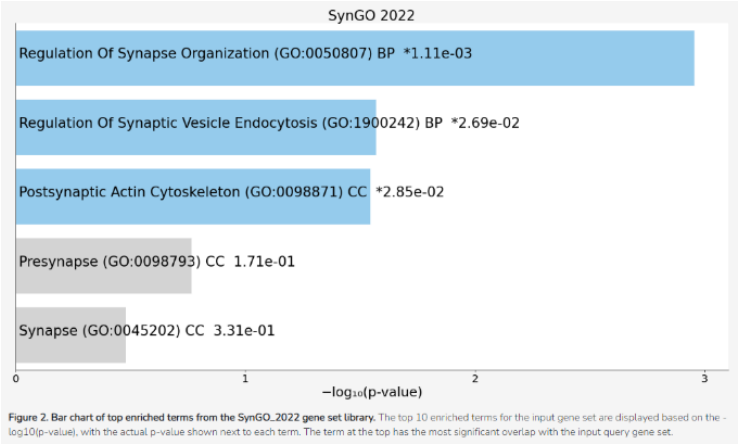

Fig. S11. Analysis of protein alterations following ketamine injection with connections to synaptic changes related to mental diseases. (**A**) Utilization of the Enrichr DisGeNET library to reveal associations with schizophrenia and bipolar disorder among the 231 altered proteins from a total pool of 517. (**B**) Construction of a Protein-Protein Interaction (PPI) network with the top 20 hub proteins from all 517 altered proteins using tools available within the Enrichr database. (**C**) Inspection of the altered proteins participating in the retrograde endocannabinoid signaling pathway according to the KEGG pathway database [45,46]. (**D**) Enrichment analysis via Enrichr-KG for proteins related to Electroconvulsive Therapy (ECT) within the disease category. (**E**) SynGO analysis identifying the cellular localization of proteins relevant to ECT.

The legends of the excel Supplementary Tables

excel Supplementary Table S1: The table reveals the altered proteins after ketamine injection, demonstrating both increased and decreased proteins that align with synapse-associated proteins outlined in the SynGO library and provided by van Oostrum *et al*.

excel Supplementary Table S2: The table presents the cellular component information of the altered proteins, encompassing both increased and decreased proteins following ketamine injection.

excel Supplementary Table S3: The table includes Biological Process ontology terms associated with the altered proteins, covering both increased and decreased proteins following ketamine injection.

excel Supplementary Table S4: The table includes records from the UP_SEQ_FEATUREs chart, a subcategory of the Functional Annotation Chart from DAVID informatics sources, for altered proteins. This encompasses both increased and decreased proteins following ketamine injection, as well as randomly chosen proteins unaffected by the ketamine injection.

excel Supplementary Table S5: The table highlights disease enrichment among all 517 altered proteins using the DisGeNET library.

excel Supplementary Table S6: The table displays the Functional Annotation Chart of all 517 altered proteins obtained from the DAVID informatics sources.

excel Supplementary Table S7: The table presents the HUB proteins identified using the ZS Revelen-PPI tool.

excel Supplementary Table S8: The table unveils 231 proteins associated with diseases out of the 517 altered proteins. Furthermore, it specifies the proteins linked to schizophrenia, Alzheimer's disease, Parkinson's disease, and bipolar disorder within the subset of 231 disease-associated proteins.

excel Supplementary Table S9: The table presents the HUB proteins identified from the enrichr tool.

excel Supplementary Table S10: The table displays plasticity-related terms associated with all 517 altered proteins, obtained from various categories within the DAVID informatics sources.